



4-3-4

EVALUATION OF LIQUEFACTION STRENGTH OF SAND BY USING CONE PENETRATION TEST

Fusao TANIZAWA¹⁾, Kimitoshi IWASAKI²⁾, Shengen ZHOU³⁾
and Fumio TATSUOKA⁴⁾

- 1) Technology Research Center, Taisei Corporation, Totsuka-ku, Yokohama, Japan
- 2) Center of Soil Engineering, Kisojiban Consultants Co. Ltd., Ohta-ku, Tokyo, Japan
- 3) China Academy of Railway Science, Beijing, China
- 4) Institute of Industrial Science, University of Tokyo, Minato-ku, Tokyo, Japan

SUMMARY

In order to investigate the relationship between the cone penetration resistance and the liquefaction strength of sand, a series of cone penetration tests has been performed in model sand deposits made in a calibration chamber, and their results were compared with the liquefaction strength obtained from torsional simple shear tests in which irregular loading patterns were used as input cyclic shear stresses. The relationship obtained by the present laboratory study was found to be well in accordance with those proposed by other researchers based on field behavior during past earthquakes.

INTRODUCTION

The cone penetration test (CPT) is a simpler and faster sounding method than the standard penetration test and is capable of obtaining continuous rather reliable information of deposits. Consequently, it has become used increasingly in surveys of reclaimed and soft grounds, supplementing or even replacing the standard penetration test. Thus studies into the method of evaluating liquefaction potential of sand using the cone penetration test results have been performed by several researchers (Refs. 1,2,3,4). However, the empirical relationships between cone penetration resistances and liquefaction strengths for sands obtained from these studies are primarily based on the field behavior of sites during past earthquakes, not based on their direct correlation in which the both were measured directly under the similar conditions.

In view of the above, a series of cone penetration tests has been performed in model sand deposits made in a calibration chamber with known liquefaction strength of the test sand.

TEST METHOD

Calibration Chamber and Cone The calibration chamber used in the present study for the cone penetration test has the dimensions of 790mm in inner diameter and 925mm in depth (Fig. 1). The horizontal and vertical stresses to the model sand deposit can be controlled independently by water pressure via rubber membranes provided on the inner peripheral face and bottom face. Further, as steel plates with thorough thickness are used for the side wall and upper/bottom plates of the cell, it is also possible to perform one-dimensional compression by making undrained the de-aired water filled between membranes and steel plates.

The cone used for testing is capable of measuring the tip resistance q_c , the sleeve friction f_s and pore water pressure u_d with the apex angle = 60° , the sectional area = 10 cm^2 , and the surface area of the friction sleeve = 100 cm^2 . These dimensions are widely employed in Japan.

Sample Preparation Toyoura sand, which is a uniform clean sand with almost no fines, was used. The specific gravity G_s is 2.64, the mean diameter D_{50} is 0.16 mm, and the maximum and minimum void ratios are $e_{\max} = 0.977$ and $e_{\min} = 0.605$ respectively. This sand has been used extensively for the laboratory studies into liquefaction of sand in Japan.

The model sand deposits were prepared by air-pluviation method using multiple sieve (Ref.5). Then the sample was consolidated one-dimensionally as follows. Firstly, anisotropic consolidation with horizontal stress $\sigma_h = 0.4 \sigma_v$ was conducted up to $1/2$ the prescribed vertical consolidation stress σ_{v0} , and then the de-aired water filled between membranes and side steel wall was made undrained and the vertical stress only was raised under the K_0 condition. Except one test on saturated sand, all the other tests were performed using air-dried sand. Effects of wet condition on q_c were found insignificant.

Cone Penetration The cone penetration tests were all performed under the drained condition and the penetration rate was 1 cm/sec. Concerning the boundary conditions between the sample and the calibration chamber, combinations as shown in Table 1 can be considered (Ref.6). Effects of the boundary condition on the cone penetration resistance are affected by the relative density of the sample and the ratio of the cone diameter to the inner diameter of the chamber (Refs.6,7). However, which of these boundary conditions or another is the most representative of the field condition is still a controversial problem. In the present study, both B2 and B3 conditions were employed.

CONE PENETRATION TEST RESULTS

Cone Penetration Characteristics Since the cone penetration resistances measured near the top and bottom boundaries were apparently influenced by the boundary conditions effects, the values of q_c averaged for $z = 40 \sim 55 \text{ cm}$ were used in the following.

Fig. 2 shows the relationships between q_c and the relative density D_r under the B2 and B3 conditions obtained from tests conducted with an initial vertical

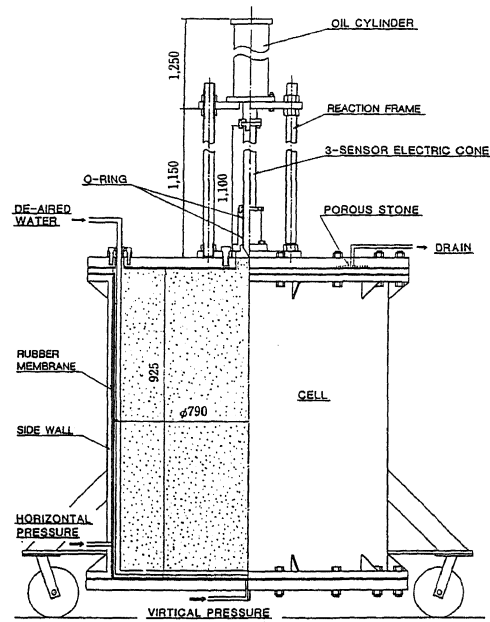


Fig. 1 Calibration Chamber

Table 1 Boundary Conditions (Ref.6)

Boundary Condition	Side Restraint	Base Restraint
B 1	Constant Stress ($\sigma_h = \text{const.}$)	Constant Stress ($\sigma_v = \text{const.}$)
B 2	Constant Volume ($de_h = 0$)	Constant Volume ($de_v = 0$)
B 3	Constant Volume ($de_h = 0$)	Constant Stress ($\sigma_v = \text{const.}$)
B 4	Constant Stress ($\sigma_h = \text{const.}$)	Constant Volume ($de_v = 0$)

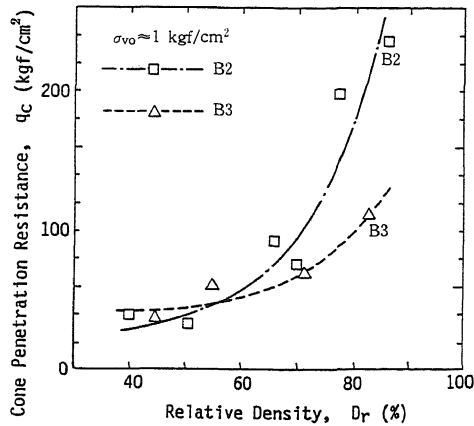


Fig. 2 q_c versus D_r

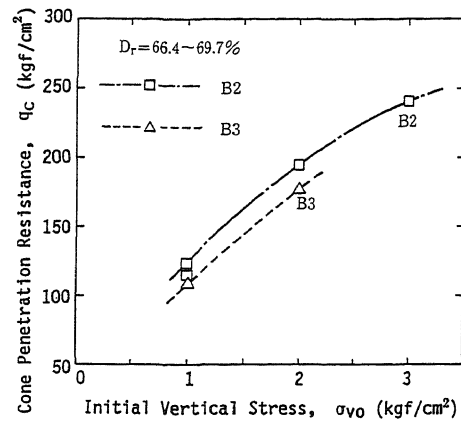


Fig. 3 q_c versus σ_{vo}

stress $\sigma_{vo} \approx 1.0 \text{ kgf/cm}^2$. The penetration resistance increases clearly with the increase in the relative density. Also, there are effects of boundary conditions, that is, the penetration resistance is larger under the B3 condition than the B2 condition for very loose sand, whereas the relations are reversed as the density increases. Fig. 3 shows the effects of the initial vertical stress σ_{vo} on the penetration resistance for medium dense samples. While q_c increases with the increase in σ_{vo} , the rate of increase tends to reduce as σ_{vo} increases.

Fig. 4 shows the relationship between the change in the vertical stress $\Delta\sigma_v$ during penetration and the relative density D_r in the case of B2 condition. $\Delta\sigma_v$ was defined at the depth where q_c was defined. It is understood that $\Delta\sigma_v$ is largely dependent on the relative density, but is only slightly affected by the initial vertical stress. In particular it should be noted that $\Delta\sigma_v$ is negative for $D_r < 50\%$ whereas $\Delta\sigma_v$ is positive for $D_r > 50\%$. It is considered that when the cone is penetrated under the condition which does not allow the volume change of the sample (B2 condition), the model sand deposit tends to contract exceeding the volume of the penetrated cone and rod in the case of a very loose sample, and tends to dilate together with the increase in the volume of the cone and rod in the case of a dense sample.

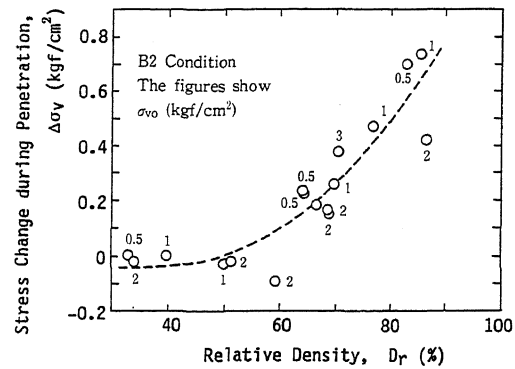


Fig. 4 $\Delta\sigma_v$ versus D_r

Relationship between Cone Penetration Resistance and Relative Density

As described above, differences of the penetration resistance between B2 and B3 conditions can be attributed to the different stress variations during penetration.

Bellotti et al. (Ref. 7) showed that the relations between the relative density of sand and cone penetration resistance and vertical stress can be represented in Eq.(1) for a coarse sand, Ticino sand.

$$D_r = a + b \log(q_c / \sigma_v^c) \quad (1)$$

where a , b and c are constants. Bellotti et al. obtained $c=0.558$ from the relations between q_c and σ_v of sand with the same relative density. A similar value was obtained in the present study. In order to simplify the equation, a power

$c=0.5$ will be used. Then the relations of the normalized cone penetration resistance and relative density have been obtained as shown in Fig. 5. Here, the value of the vertical stress includes the change during penetration (see Fig. 4). A unique relationship irrespective of boundary conditions, B2 and B3, unlike the result shown in Fig. 2, was obtained. This relation is approximately expressed as

$$D_r = -85.0 + 76.2 \log(q_c / \sigma_v^{0.5}) \quad (2)$$

or more precisely as

$$D_r = 154 - 182 \log(q_c / \sigma_v^{0.5}) + 68 [\log(q_c / \sigma_v^{0.5})]^2 \quad (3)$$

where, the unit of D_r is in %, and those of q_c and σ_v are in kgf/cm^2 .

LIQUEFACTION STRENGTH AND CONE PENETRATION RESISTANCE

Liquefaction Strength Fig. 6 shows the relationships between the relative densities and undrained resistances of isotropically consolidated Toyoura sand specimen prepared by air-pluviation method as used for the calibration chamber CPTs. These results were obtained by the cyclic torsional simple shear (CTSS) test (Ref. 8). The time histories of acceleration measured at the ground surface at an epicentral distance $\Delta = 189$ km during the main shock (shock-type) and at $\Delta = 193$ km during the largest after shock (vibration-type) of the Tokachi-oki earthquake of 1968 were used as input irregular time histories of shear stresses τ . The liquefaction strength was defined by a maximum double amplitude shear strain $DA_{max} = 15\%$, in terms of the ratio of the maximum single amplitude shear stress τ_{max} and the initial mean effective stress σ_{mc}' . Also in Fig. 6, the liquefaction strength defined by a double amplitude shear strain $DA_{max} = 15\%$ obtained using uniform cyclic shear stresses is shown. For low relative densities, the relations expressed by broken lines were extrapolated based on the results by the uniform loading tests.

Fig. 7 shows the result of the cyclic undrained triaxial (CTX) test conducted on the Toyoura sand used for the CPT. In Fig. 7, the horizontal axis represents the number of loading cycles to a double amplitudes axial strain $DA = 10\%$. The figure also shows the result of the simi-

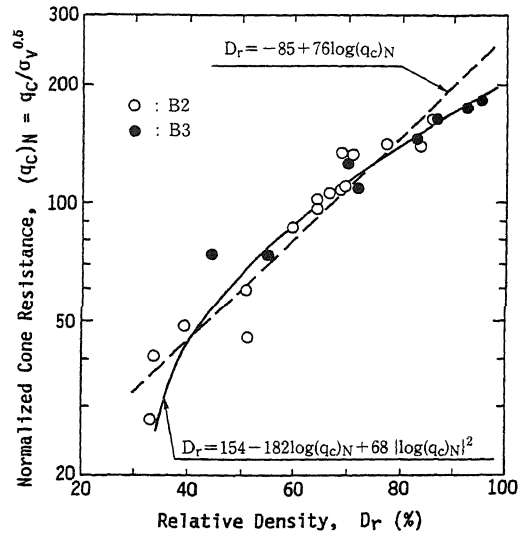


Fig. 5 $q_c / \sigma_v^{0.5}$ versus D_r

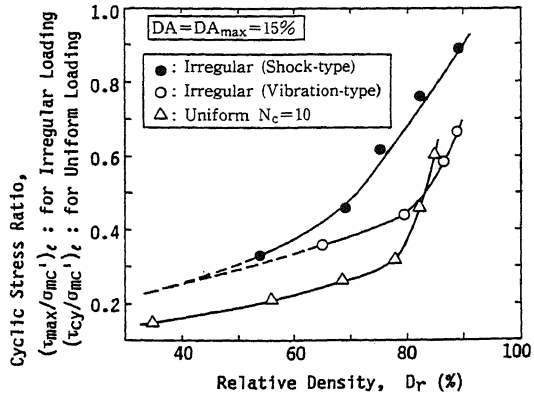


Fig. 6 Liquefaction strength by CTSS versus D_r

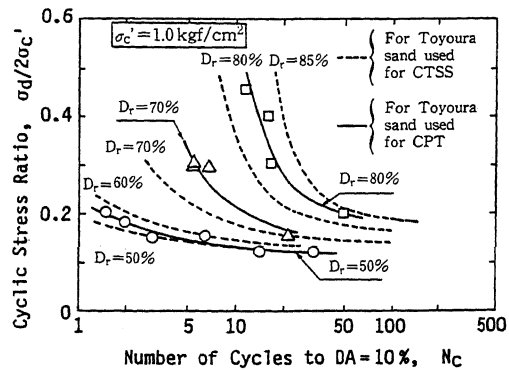


Fig. 7 Liquefaction strength by CTX

lar tests using the same Toyoura sand as used for the CTSS test (Ref. 9). Though the same apparatus was used, there are slight differences in the results unfortunately, indicating that the liquefaction strength is generally larger for the Toyoura sand specimen used in the CPT.

From the above, before the results shown in Fig. 6 were used for defining the correlations of the liquefaction strength and cone penetration resistance, the relative density values D_{r2} of Toyoura sand used in CTSS test, equivalent to that used for the CPT (D_{r1}), were obtained by using the relationship shown in Fig. 8; i.e., each sets of relative density values D_{r1} and D_{r2} for each data point in Fig. 8 correspond to the same liquefaction strength by the CTX test shown in Fig. 7.

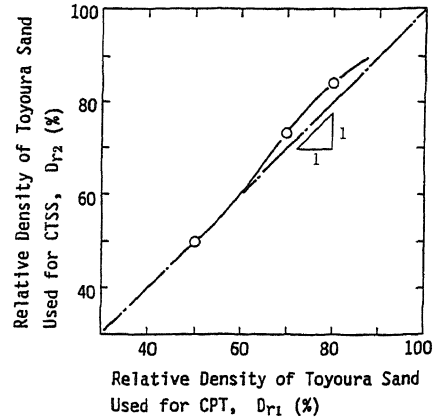


Fig. 8 Equevalent relative density values of two sorts of Toyoura sand

Relationships of Cone Penetration Resistance and Liquefaction Strength

The relationships between the liquefaction strength for the irregular loading and the cone penetration resistance q_{c1} at $\sigma_v = 1 \text{ kgf/cm}^2$, shown in Fig. 9, were obtained as follows. First, the value of q_{c1} for a certain value of D_{r1} was obtained from Eq. (3). Then, the value of D_{r2} corresponding to this value of D_{r1} was obtained from the relationship shown in Fig. 8. Then, the values of liquefaction strength for D_{r2} were obtained from the relationships shown in Fig. 6. It should be noted, however, that the isotropic consolidation applied in the CTSS test, which is different from the K_0 consolidation applied in the CPT, the liquefaction strength in terms of (τ_{\max}/σ_v') assumed to be a value of $(\tau_{\max}/\sigma_{mc}')$ multiplied by $(1+2K_0)/3$. Here, K_0 was calculated by using the relation $K_0 = 0.52e$ (e : void ratio) proposed by Okochi and Tatsuoka (Ref. 10).

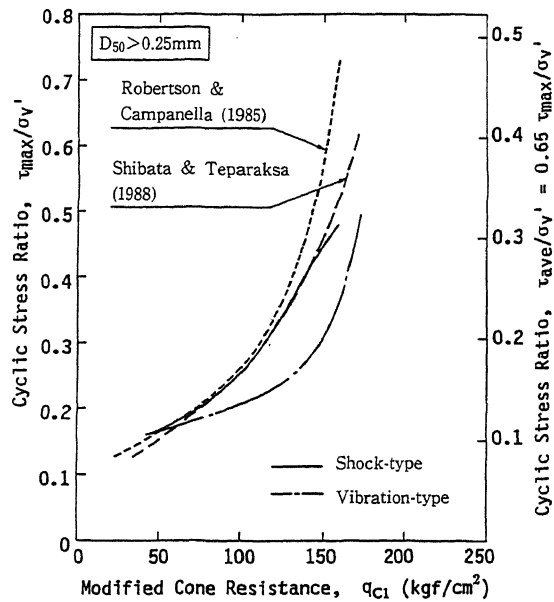


Fig. 9 Liquefaction strength versus q_{c1}

The dotted line and broken line shown in Fig. 9 represent respectively the relations of q_{c1} and $(\tau_{\max}/\sigma_v') = (\tau_{\text{ave}}/\sigma_v')/0.65$ for clean sands having mean grain size $D_{50} > 0.25 \text{ mm}$ proposed by Robertson and Campanella (Ref. 3) and Shibata and Teparaksa (Ref. 4) based on field behavior during past earthquakes. Since Toyoura sand is uniform clean sand including no fines in spite of its small value of $D_{50} = 0.16 \text{ mm}$, these relationships are shown in the same figure.

The relationships between the liquefaction strength and the cone penetration resistance in the present study were obtained under very limited conditions; i.e., they were obtained from the results of laboratory test using a single kind of sand. Therefore, it is not available for the general use. However, as seen from Fig. 9, the relationship for the shock-type shows favorable coincidence with

those proposed by taking into account the actual liquefaction phenomena. The result appears to indicate the possibility of evaluation of in-situ liquefaction strength by using the relations obtained from the results of laboratory test by using the method as is used in the present study.

CONCLUSIONS

From the results of laboratory test for Toyoura sand obtained by the present study, the followings were obtained;

- (1) The cone penetration resistances measured in samples made in the calibration chamber were influenced by relative density, vertical stress and also the boundary conditions.
- (2) While different penetration resistances q_c were obtained for the two different boundary conditions for the same initial stress condition, a unique relation between q_c and the vertical stress σ_v was obtained when the values of σ_v during penetration were used in the above relation.
- (3) q_c increased proportionally to $\sigma_v^{0.5}$. Thus, an empirical relationship between the relative density and $q_c/\sigma_v^{0.5}$ was obtained.
- (4) The relationship between the cone penetration resistance and the liquefaction strength of Toyoura sand obtained by the present laboratory study was found to be well in accordance with those which have been proposed based on the field behavior during past earthquakes.

ACKNOWLEDGMENTS

This study was performed at Institute of Industrial Science, University of Tokyo while Mr. Zhou was staying at the institute as Visiting Research Personnel. The authors would like to express their appreciation to Mr. Takeshi Sato and Mr. Jong Chul Im for their cooperations during the present study.

REFERENCES

1. Zhou, S.; Evaluation of the Liquefaction of Sand by Static Cone Penetration Test, Proc. of the 7th WCEE, Vol.3, (1980).
2. Seed, H.B., Idriss, I.M. and Arango, I.; Evaluation of Liquefaction Potential Using Field Performance Data, Journal of Geotechnical Engineering, ASCE, Vol.109, No.3, (1983).
3. Robertson, P.K. and Campanella, R.G.; Liquefaction Potential of Sands Using the CPT, Journal of Geotechnical Engineering, ASCE, Vol.111, No.3, (1985).
4. Shibata, T. and Teparaksa, W.; Evaluation of Liquefaction Potentials of Soils Using Cone Penetration Tests, Soils and Foundations, Vol.28, No.2, (1988).
5. Miura, S. and Toki, S.; A Sample Preparation Method and its Effect on Static and Cyclic Deformation-Strength Properties of Sand, Soils and Foundations, Vol.22, No.1, (1982).
6. Parkin, A.K. and Lunne, T.; Boundary Effects in the Laboratory Calibration of a Cone Penetrometer for Sand, Proc. of the 2nd ESOPT, Vol.2, (1982).
7. Bellotti, V. et al.; Laboratory Validation of In-situ Tests, Geotechnical Engineering in Italy, (1985).
8. Tatsuoka, F., Maeda, S., Ochi, K. and Fujii, S.; Prediction of Cyclic Undrained Strength of Sand Subjected to Irregular Loadings, Soils and Foundations, Vol.26, No.2, (1986).
9. Tatsuoka, F., Ochi, K., Fujii, S. and Okamoto, M.; Cyclic Undrained Triaxial and Torsional Shear Strength of Sands for Different Sample Preparation Methods, Soils and Foundations, Vol.26, No.3, (1986).
10. Okochi, Y. and Tatsuoka, F.; Some Factors Affecting K_0 -values of Sand Measured in Triaxial Cell, Soils and Foundations, Vol.24, No.3, (1984)